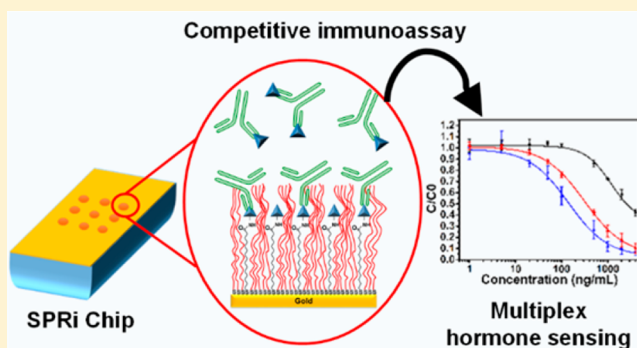


Multiplex Surface Plasmon Resonance Imaging-Based Biosensor for Human Pancreatic Islets Hormones Quantification

F. Rafael Castiello[†] and Maryam Tabrizian^{*,†,‡,§}[†]Biomedical Engineering Department and [‡]Faculty of Dentistry, McGill University, Montreal, Quebec H3A 2B4, Canada

Supporting Information

ABSTRACT: Diabetes arises from secretory defects in vascularized micro-organs known as the islets of Langerhans. Recent studies indicated that furthering our understanding of the paracrine effect of somatostatin on glucose-induced insulin secretion could represent a novel therapeutic avenue for diabetes. While many research groups are interested in insulin and glucagon secretion, few are particularly focused on studying the paracrine interaction in islets' cells, and none on monitoring a secretory fingerprint that contemplates more than two hormones. Surface plasmon resonance imaging can achieve high-throughput and multiplexed biomolecule quantification, making it an ideal candidate for detection of multiple islet's secretion products if arrays of hormones can be properly implemented on the sensing surface. In this study, we introduced a multiplex surface plasmon resonance imaging-based biosensor for simultaneous quantification of insulin, glucagon, and somatostatin. Performing this multiplex biosensing of hormones was mainly the result of the design of an antifouling sensing surface comprised by a mixed self-assembly monolayer of CH₃O-PEG-SH and 16-mercaptohexadecanoic acid, which allowed it to operate in a complex matrix such as an islet secretome. The limit of detection in multiplex mode was 1 nM for insulin, 4 nM for glucagon, and 246 nM for somatostatin with a total analysis time of 21 min per point, making our approach the first reporting a label-free and multiplex measurement of such a combination of human hormones. This biosensor holds the promise of providing us with a mean for the further understanding of the paracrine effect of somatostatin on glucose-induced insulin secretion and consequently help develop novel therapeutic agents for diabetes.



Diabetes mellitus affects 12.9% of the adult population in North America and the Caribbean region, from which type 2 diabetes (T2D) accounts for 90–95% of the cases.¹ Diabetes arises from secretory defects in the pancreatic islets of Langerhans, which are endocrine clusters of cells with an average diameter of 150 μm .² The islets are vascularized micro-organs with five different types of cells (α , β , δ , PP, and ϵ) that cooperate for hormone secretion in response to metabolic changes.^{2,3}

Recent studies indicate that the pancreatic islet's anatomy and physiology are species-dependent and that the unique cytoarchitecture of human islets has significant consequences for cell-to-cell communication within the islets.⁴ For instance, secreted hormones from the different islets' cells may exert paracrine interaction on their neighbor cells,^{3,5,6} particularly somatostatin whose inhibition has been shown to increase glucose-induced insulin secretion.⁷ Further understanding of these paracrine effects may represent a therapeutic avenue for T2D.^{5,6}

Up until now, most of the pancreatic islet research depends on traditional bioassays for hormone quantification such as patch clamp,^{8–12} capillary electrophoresis immunoassays (CEI),^{13–16} and ELISA.^{16–18} Patch clamp has been used to study the secretion from individual islet β -cells^{8–10} and α -cells.^{11,12} This technique provides quantitative information

regarding exocytosis, by correlating the rate of capacitance change with the number of granules released at a given time.¹⁹ However, the patch clamp technique requires highly skilled operators to trap and manipulate individual cells, is low throughput, it only provides an indirect measurement of secretion, and it lacks specificity for individual secretion products. On the other hand, CEI has been used for direct detection of insulin¹⁴ and glucagon¹⁵ from pancreatic islets. During CEI experiments, islets are placed in a chamber and the effluent is mixed with the targeted hormone antibodies and fluorescent-labeled hormones. The secreted hormones from the islets then compete with fluorescent-labeled hormones for binding sites on the antibody. This mixture is then passed into an electrophoresis channel where bound and unbound fluorescent hormones are separated. Hormone secretion is then quantified fluorescently by establishing the ratio between bound and free hormone. As with patch clamp, CEI requires skilled operators to work effectively, precise temperature control, overcoming channel clogging, and the integration of lasers with different wavelengths.¹⁵ Finally, although operation-

Received: October 17, 2017

Accepted: January 29, 2018

Published: January 29, 2018

ally simpler, ELISA is difficult to use for simultaneous quantification, is time-consuming, and is expensive. Moreover, all the mentioned techniques face many challenges when trying to expand them for simultaneous analysis of multiple targets.

While many research groups are interested in insulin and glucagon secretion,^{20–23} few are particularly focused on studying the paracrine interaction in islets' cells,⁵ and none on monitoring a secretory fingerprint (SF) for more than two hormones. Hence, to monitor an islets' SF, implementation of multiplexed analytical tools is required.

In this context, surface plasmon resonance imaging (SPRi) could be a useful tool to measure a pancreatic islet's SF. SPRi is now established as the gold standard to study biomolecular interactions such as antigen–antibody.²⁴ In addition to label-free and real-time analysis, SPRi can achieve high-throughput and multiplexed measurements through arrays of different molecules on the sensing surface.²⁴ In the past decade, SPR biosensors have mostly been used to investigate fundamental physiological aspects of the major secreted islet hormones, namely, insulin,^{25–27} somatostatin,²⁸ pancreatic polypeptide,^{29,30} and ghrelin.³¹ However, there are no reports of a SPRi multiplex biosensor aiming to dynamically quantify more than two of the major secreted hormones. SPRi biosensors present an additional advantage for this particular application that involves measurements in a complex matrix such as the islet secretome. This advantage is provided by designing antifouling surfaces using self-assembled monolayers (SAM) that reduce interferences caused by nonspecific adsorption of molecules on the sensor surface.³²

Here in, we introduce an SPRi-based biosensor for multiplexed detection of insulin, glucagon, and somatostatin. First, we studied the effect of composition on the antifouling properties of a mixed SAM of a thiolated polyethylene glycol (CH₃O-PEG-SH) and 16-mercaptohexadecanoic acid (MHDA). The antifouling properties of the biosensor were investigated by injecting two proteins: bovine serum albumin (BSA) and lysozyme (LYZ). Next, a competitive immunoassay protocol for insulin, glucagon, and somatostatin was implemented, and the biosensor performance for individual hormones was determined. Finally, the biosensor performance was tested in multiplex mode performing simultaneous competitive immunoassays for the three hormones, and the limit of detection (LOD) and dynamic range were determined for each hormone in the mixture.

EXPERIMENTAL SECTION

Materials and Apparatus. Absolute ethanol was purchased from Fisher Scientific (Fair Lawn, NJ), and phosphate-buffered saline (PBS) tablets, Tween 20, and glycine were purchased from BioShop Canada Inc. (Burlington, Ontario, Canada). Ethanolamine hydrochloride, *N*-(3-(dimethylamino)propyl)-*N'*-ethylcarbodiimide hydrochloride (EDC), *N*-hydroxysuccinimide (NHS), bovine serum albumin (BSA), hydrochloric acid (HCl), human glucagon, human somatostatin, and lysozyme (LYZ) were purchased from Sigma-Aldrich (St. Louis, MO). Tris-buffered saline (TBS) with 1% casein was purchased from BIO-RAD. Anti-insulin antibody (6.2 mg/mL) and human insulin were purchased from PROSPECT (Ness, Ziona, Israel). Anti-glucagon and anti-somatostatin antibodies (200 µg/mL each) were purchased from Santa Cruz Biotechnologies, Inc. (Mississauga, ON, Canada). CH₃O-PEG-SH (MW 1200 Da) was purchased from Rapp Polymere GmbH (Tübingen, Germany). 16-Mercaptohexadecanoic acid

(MHDA) was purchased from ProChimia Surfaces Sp. (Zacisze, Sopot, Poland).

SPRi detection was performed using a scanning-angle SPRi instrument (model SPRi-Lab+, Horiba, France). The SPRi apparatus, equipped with an 800 nm LED source, a CCD camera, and a microfluidic flow cell, was placed in an incubator at 25 °C (Memmert Peltier, Rose Scientific, Canada).

SPRi Measurements. For all experiments, the slope of the plasmon curves was automatically computed by the instrument's software to facilitate the selection of the working angle for kinetic analysis. This slope corresponds to the point of the plasmon curve at which the slope was maximum. Reflectivity shift (ΔR (%)) for all experiments was acquired upon stabilization of the baseline. Measured values were the average of at least three spots for each sample including controls, and each experiment was repeated at least three times. At each step, the substrate was washed with the running buffer PBS-T (PBS with 0.002% Tween 20), and the difference in the reflected intensity was measured by taking into account the difference between the initial and final buffer signal. An injection loop with a fixed volume of 200 µL was used during the experiments. A flow rate of 20 µL/min was used for all experiments, with the exception of functionalization steps where the flow rate was adjusted depending on the required contact time.

Substrate Preparation. For single hormone-sensing, cleaned microscope glass slides (12 mm × 25 mm × 1 mm, $n = 1.518$) substrates were coated with 2 nm Cr as an adhesion layer, followed by the deposition of a thin Au layer of 48 nm using electron-beam physical vapor deposition under high vacuum. Microscope glass slides were then coupled to an SF11 equilateral triangular prism ($n_{\text{SF-11}} = 1.765$) using a refractive index matching liquid. For multiplex sensing, similar gold-coated prisms ($n = 1.765$) purchased from Horiba Scientific-GenOptics, France, were used as received.

Surface Functionalization. Substrates were cleaned by subsequent immersion in absolute ethanol and deionized (DI) water and dried with a stream of nitrogen. Ethanolic solutions of 0.5 mM CH₃O-PEG-SH and 0.5 mM MHDA were prepared and mixed at different molar ratios from 100% MHDA to 90% CH₃O-PEG-SH–10% MHDA. Substrates were immersed in the above-mentioned ethanolic solutions overnight to allow the self-assembly monolayer (SAM) formation. Finally, the substrates were thoroughly rinsed with absolute ethanol and DI water and dried under a stream of nitrogen.

Microscope slides with freshly prepared SAMs were immediately placed on the SPRi system for subsequent functionalization. First, conditioning was performed by 4 serial injections (contact time of 2 min each) of a regeneration solution containing 1 M glycine pH 2.5 (1M-Gly). Then, the surface was rinsed with PBS-T until the baseline was stable. Next, NHS/EDC chemistry was used to covalently bind insulin, glucagon, or somatostatin as reported by Gobi et al.³³ Briefly, 200 µL of an aqueous solution containing 2 mg/mL NHS, 2 mg/mL EDC, and 50 µg/mL of the desired hormone were flowed over the sensor with a contact time of 1 h. Next, an injection of 200 µL (contact time 10 min) of 1 M ethanolamine hydrochloride pH 8.5 was performed to inactivate unfunctionalized –COOH groups on the sensor surface. Then, two serial injections of regeneration solution (contact time 1 min each) were performed to remove weakly bound hormones. Finally, a blocking solution containing 1% casein and 5% BSA in TBS buffer was injected with a contact time of 30 min, and subsequently, at least 3 injections of the regeneration solution

were made to remove weakly bound proteins. Figure 1 shows a graphical representation of a typical sensor functionalization.

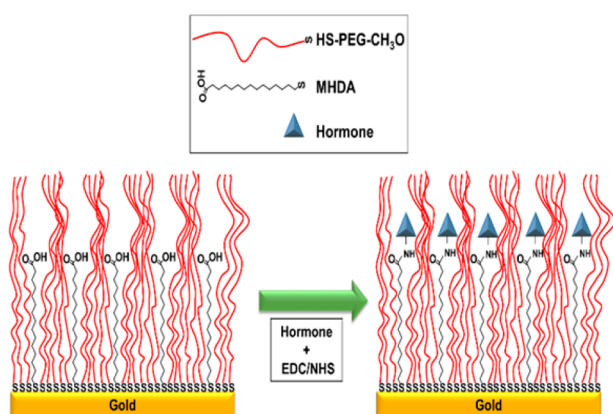


Figure 1. Schematic representation of the surface functionalization of thin Au films used in this study. The surface is composed of a mix SAM of 16-mercaptohexadecanoic (MHDA) as a linker and a thiolated PEG ($\text{CH}_3\text{O-PEG-SH}$) as a spacer and antifouling agent incubated overnight. Targeted hormones are covalently immobilized to the surface using EDC/NHS chemistry in an aqueous solution.

For the functionalization of gold-coated prisms in multiplex measurement mode, the procedure described for microscope slides was followed with some minor changes. After conditioning, 4 individual solutions containing NHS/EDC (2 mg/mL each) and 50 $\mu\text{g/mL}$ of insulin, glucagon, somatostatin, or BSA were spotted (150 nL) in triplicate on the surface of the prism and incubated in a humidity chamber for 1 h. Immediately after, the prism was rinsed with a copious amount of DI water and subsequently immersed in 1 M ethanolamine hydrochloride pH 8.5 for 10 min. Next, the prism was immersed in the blocking solution for 30 min, subsequently rinse with DI water and placed in the SPR flow chamber. Then, the regeneration solution was injected at least three times to obtain a stable baseline before beginning with the competitive immunoassays.

Competitive Immunoassay. For multiplex assays, standard solutions containing insulin, glucagon, and somatostatin were prepared in PBS-T buffer at a concentration range of 1–4000 ng/mL and mixed with a cocktail of antibodies containing anti-insulin (1 $\mu\text{g/mL}$), anti-glucagon (2 $\mu\text{g/mL}$), and anti-somatostatin (2 $\mu\text{g/mL}$). These mixtures were incubated for 2 min under gently mixing and serially injected over the spotted sensor chip from highest to lowest hormone concentration (contact time of 10 min) starting with a blank solution containing only the antibody cocktail. Each sensing cycle comprised: sample injection 10 min, 5 min buffer washing, and 2 injections of regeneration solution (1M-Gly) with a contact time of 25 s with 3 min washing with buffer in-between. For individual immunoassays, the same conditions were used, with the exception of somatostatin, for which the assay concentration ranged from 50 to 8000 ng/mL. For all competitive immunoassays, the optimal antibody concentration was defined as the concentration that could generate a small but detectable SPR signal of $\Delta R \approx 1$, which has been previously reported as a reliable ΔR for this type of assays.³⁴

Statistics. For all competitive immunoassays, relative binding (C/C_0) was calculated by dividing the response of the standard solutions containing hormones (C) by the

response of the blank solution containing only a fixed concentration of antibodies (C_0). To generate calibration curves C/C_0 was plotted against hormone concentration. The calibration curves were fitted using a nonlinear 4 parameter logistic (4PL) model. The lower limit of detection (LOD) for all immunoassays was calculated from the calibration curves as the blank signal (C_0) minus 3 times the standard deviation. The dynamic range for the competitive immunoassay was established between $0.2C/C_0$ and $0.8C/C_0$. All data is expressed as the average of at least 3 independent experiments \pm standard deviation (SD).

RESULTS AND DISCUSSION

Effect of SAM Composition on the Sensor Response.

SAMs are typically used as a linker layer for immobilization of biological components at the transducer surface of biosensors.³² A necessary procedure when developing a competitive immunoassay is limiting the amount of competing antigen and antibody in order to maximize the assay's sensitivity. Typically, commercial SPR chips achieve this by fixing the SAM composition and controlling the surface density of the analyte, either by changing the contact time or the concentration of the analyte during functionalization.³⁵ However, in a mass-sensitive technique such as SPR, the detection of small molecules (such as the target peptides in this study) is challenging, requiring careful design of the surface chemistry to ensure optimal sensitivity.³⁶ Thus, the linker to spacer ratios must be studied in detail on a case basis.

In this work, a mixed SAM comprised of a linear thiol with a carboxyl end group (MHDA) was used for hormone immobilization, along with a low molecular weight thiolated PEG ($\text{CH}_3\text{O-PEG-SH}$) that acts as a spacer and as an antifouling agent.³⁷ These compounds are used on a regular basis for biosensor development; however, this work presents the first report using them in combination. Additionally, contrary to the majority of the reports in the literature,³² our study presents a long chain compound as a spacer and a short chain as an anchor. Thus, the results obtained could be counterintuitive when compared to previous reports. In addition, SAM composition plays an important role on the final surface density of immobilized biomolecules; thus, a preliminary study was performed to evaluate its effect on the sensor's response. Since somatostatin was the smallest of the targeted hormones, it was used as the "reference" hormone for this study.

Figure 2 shows the change in reflectivity for a fixed amount of antisomatostatin antibodies (1 $\mu\text{g/mL}$) over different SAM compositions. With 100% and 50% MHDA, a large signal can be observed. Interestingly a change occurred after 50% PEG molar fraction, the signal abruptly diminished and it was barely present for the 70% and 90% PEG molar fractions. This could be explained by the fact that mixtures of *n*-alkanethiols of different chain lengths tend to form SAMs with a composition enriched with the longer alkanethiol.³² Thus, a very little amount of linker is left on the surface to covalently bind somatostatin.

For 70% and 90% PEG molar fractions, it was necessary to increase 20–30 times the antisomatostatin antibody concentration to obtain a measurable SPR signal. This presents some disadvantages for the sensor operation for the following reasons: (1) for a competitive immunoassay, a large amount of antibodies will be poorly inhibited by a small amount of analytes.³⁸ (2) Each data point in this type of assay requires the

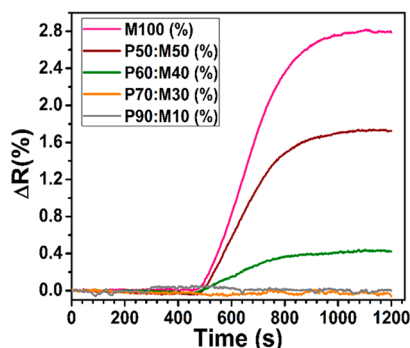


Figure 2. SPR reflectivity change response of 1 $\mu\text{g/mL}$ of antisolomatostatin antibody for different SAM compositions. P and M stand for $\text{CH}_3\text{O-PEG-SH}$ and MHDA, respectively.

injection of a fresh antibody solution; hence, a high amount of antibodies will increase reagent consumption and operational costs.

On the other hand, 100% and 50% MHDA surface regeneration proved to be challenging when compared to 40% MHDA (Figure S1). Thus, we set the final composition of SAM as 60% PEG–40% MHDA to incorporate the maximum amount of PEG and still get a detectable signal, even with a relative low antibody concentration.

Single-Step Hormone Immobilization. The hormones used in this work are small peptides possessing an N-terminal group which could be used for immobilization on the sensor surface, through an amide bond formation with the carboxyl group on the MHDA. The surface functionalization was performed in a single step as reported by Gobi et al.³³ Compared to typical two-step NHS/EDC processes where buffer solutions with a variety of pH are required,^{39,40} the single step functionalization offers the advantage of reducing the functionalization time and pH adjustments for all hormones since the reaction is performed in aqueous solution. This is particularly advantageous when preparing SPR surfaces using several hormones solutions.

After chip conditioning, individual hormones and the immobilization reagent (a mixture of NHS/EDC) were injected over the sensor chip. Once the solution reached the surface, the SPR angle decreased slightly followed by a steady angle increase to nearly reach a plateau representing surface saturation. At the end of the injection, the surface was washed with running buffer until a stable baseline was obtained. Finally, in order to make the sensor surface homogeneous, a blocking agent containing 5% BSA and 1% casein (w/w) in TBS buffer was injected with a total contact time of 30 min. At the end of the injection, running buffer was allowed to wash the surface until stabilization of the SPR signal occurred. After this point, at least 2 injections of regeneration solution were used to remove any weakly adsorbed BSA and casein. Once the baseline was stabilized, the difference in SPR angle before and after the blocking step was measured.

Table 1 shows the corresponding mean reflectivity change observed after the individual hormone functionalization and its corresponding blocking step ($n = 3$). Interestingly, since the available functionalization sites are fixed, the reflectivity change values for each hormone functionalization proved to be proportional to their differences in molecular weight (MW insulin > glucagon > somatostatin).

Biosensor Performance for Individual Immunoassays. Direct immunoassays of small molecules by SPR can be

Table 1. SPR Mean Reflectivity Change after Individual Hormone Functionalization and Their Corresponding Blocking Step

hormone	ΔR (%) functionalization	ΔR (%) blocking
insulin	8.26 ± 0.57	0.3 ± 0.07
glucagon	4.57 ± 0.32	0.26 ± 0.06
somatostatin	3.36 ± 0.66	0.89 ± 0.17

challenging since the SPR signal is directly related to the change in mass at the sensor surface. Consequently, the immunoassays in the present work were performed in a competitive manner where inhibition of antibody binding is due to binding occurring with hormones in solution. Thus, the higher the concentration of hormones in solution, the smaller the SPR signal and vice versa (Figure 3).

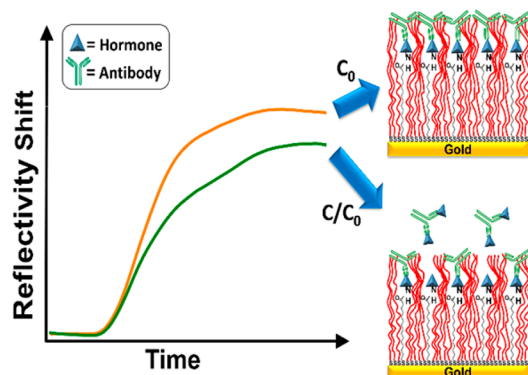


Figure 3. Graphical representation of a competitive immunoassay over the sensor surface. After formation of a mixed SAM and functionalization with the targeted hormone covalently linked to the SAM, inhibition of the blank solution with optimal antibody concentration (C_0) follows due to binding occurring with hormones in solution (C/C_0). Thus, the higher the concentration of hormones in solution, the smaller the SPR signal and vice versa.

In general, competitive immunoassays require the use of a small antibody concentration so that slight amounts of the analyte can inhibit antibody binding to the surface.³⁸ For this reason, the optimal antibody concentration for each hormone was defined as the concentration of the antibody that could generate a small but detectable SPR signal of $\Delta R \approx 1$.³⁴ This corresponded to an antibody concentration of 1, 2, and 2 $\mu\text{g/mL}$ for anti-insulin, anti-glucagon, and anti-somatostatin, respectively.

To study the sensor performance, standard solutions containing either insulin, glucagon, or somatostatin were prepared in PBS-T. Then, the optimal amount of antibody was added to the standard solution and gently mixed for a predefined period of time before injecting into the SPR system. Somatostatin was particularly sensitive to incubation conditions during this step. After testing different times and mixing conditions, it was found that 2 min incubation under gently manual agitation provided optimal conditions for sensing (data not shown).

Figure 4 shows the sensor calibration curves for insulin (Figure 4A), glucagon (Figure 4B), and somatostatin (Figure 4C). For each hormone, mean relative binding values (C/C_0) were plotted as a function of hormone concentration (ng/mL). For each experiment, the entire sensor surface was functionalized, and the mean SPR shift was measured on at least 10

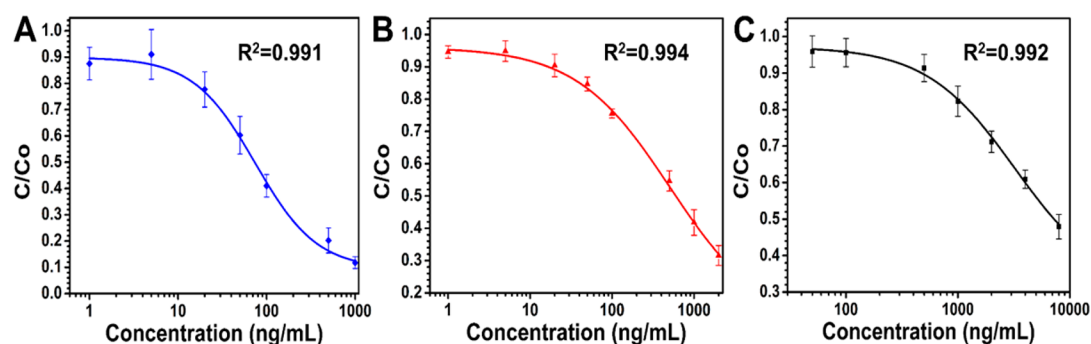


Figure 4. Individual hormone calibration curves in PBS-T for (A) insulin, (B) glucagon, and (C) somatostatin. For each hormone, mean relative binding values (C/C_0) were plotted as a function of hormone concentration (ng/mL). Relative binding was calculated by dividing the response for each concentration (C) by the response from a solution containing only the optimal concentration of individual antibodies (C_0). Solid lines correspond to the fitting of a nonlinear 4PL model. Error bars represent the standard deviation from 3 independent experiments ($n = 3$).

spots from different regions of the chip. Then, an average of these SPR shifts from three independent sensors was calculated and the bars in Figure 4 represent the corresponding SD. The LOD and dynamic range for individual immunoassays are shown in Table 2.

Table 2. SPR Sensing Performance for Single Hormones^a

hormone	ΔR (%) (C_0)	LOD (ng/mL)	LOD (nM)	dynamic range (ng/mL)
insulin	1.47 ± 0.06	12	2	15–338
glucagon	1.25 ± 0.02	4	1	72–2000 ^b
somatostatin	1.11 ± 0.03	409	250	1237–8000 ^b

^aAll values were calculated from the nonlinear 4PL fit equation derived from individual calibration curves. The reported LOD was calculated as the response of the blank (C_0) minus 3 times the standard deviation.

^bHighest concentration tested.

Additionally, we tested different sensor regeneration solutions including 10–50 mM NaOH, 10 mM NaOH 1–20% (v/v)–acetonitrile, 0.1–1 M glycine (pH 2–3), 0.1–1 M glycine–1% (v/v) DMSO, and 2 M MgCl₂, 0.1–1 M glycine–1% (v/v) DMSO, and 2 M MgCl₂ (data not shown). From these solutions, 1 M glycine with a pH = 2.5 provided the more efficient conditions for surface regeneration.

Finally, the sensor's resistance to nonspecific absorption of proteins was determined by separately injecting BSA and LYZ with a final concentration of 1 mg/mL. The injection of these solutions was performed at the end of each calibration curve experiment under the same experimental conditions as the standard solutions used during hormone sensing. The shift in reflectivity was measured after 10 min of contact time and 5 min PBS-T wash. For all cases, during BSA injection the SPR angle increased abruptly and later returned to a slightly smaller baseline value, likely due to the high bulk refractive index change during the injection. This can be interpreted as a

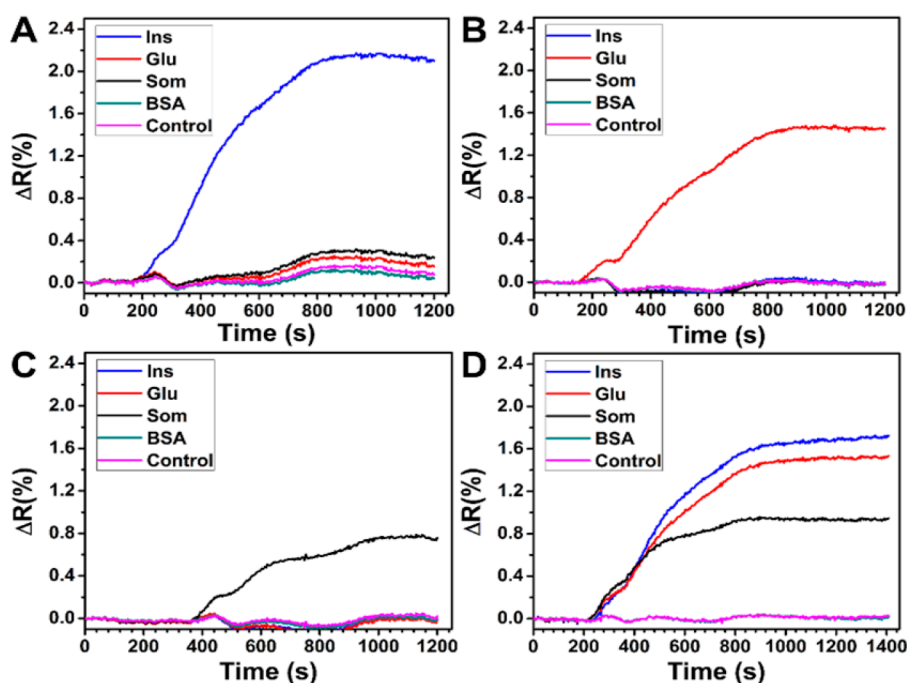


Figure 5. Spot specificity on a multiplex sensing surface for (A) anti-insulin, (B) anti-glucagon, and (C) anti-somatostatin. (D) Typical blank solution response (C_0) for multiplex immunoassays. Immobilized BSA (green line) and the bare SAM surface, identified in the graphs as “Control” (pink line), were used as negative controls.

negligible accumulation of BSA on the sensor surface. In the case of LYZ injection, the sensor registered a positive increase in the baseline value immediately after the buffer washing step. The adsorbed amount of LYZ was less than 100 pg/mm² for all hormone-functionalized surfaces. This value is consistent with the definition of an antifouling surface.³⁷ Moreover, a single injection of regeneration solution for 25 s returned the baseline to its original value, indicating a weak interaction of LYZ on the sensor's surface. Table S1 in the Supporting Information shows the mean ($n = 3$) SPR response to BSA and LYZ immediately after buffer washing

Biosensor Performance for Multiplex Immunoassays.

Multiplex hormone detection was achieved by simultaneously performing three immunoassays. Once the different hormones were immobilized on the surface and the chip blocked, the spot cross-reactivity was investigated. Figure 5 shows the sensor response to individual injection of the optimal antibody concentration of anti-insulin (Figure 5A), anti-glucagon (Figure 5B), and anti-somatostatin (Figure 5C). The typical sensor response to a blank solution (mix of all antibodies) is shown in Figure 5D. Each injection caused an increase in SPR signal on the relevant spot, indicating specific binding and low cross-contamination between the spots. A certain level signal variation was observed between individual injections of antibodies (Figure 5A–C) and the injection of the antibody mix (Figure 5D). This signal variability may arise due to subsequent injection and regeneration of the sensor's surface since the multiplex sensor presented a similar performance to that of the individual sensors, as shown later in this section. This did not represent a major drawback during the sensor operation, as we recorded consistent and reproducible measurement during all of our experiments.

For this experiment, two negative controls were used: the bare SAM surface and spots functionalized with BSA, as identified by "Control" (pink color) and BSA (green color) in Figure 5. As it can be seen in Figure 5D, there was a negligible response on the BSA and "Control" spots when exposed to the blank solution, indicating the high antifouling properties of the sensor.

To further determine the antifouling properties of the sensor in multiplex mode, separate injections of BSA and LYZ with a final concentration of 1 mg/mL were performed. As with individual sensing experiments, BSA injection resulted in a small decrease of the baseline while LYZ lead to a slight increase in the baseline value measured after buffer washing. Similarly to individual assays, the adsorbed amount of LYZ was well within the definition of an antifouling surface³⁷ (less than 100 pg/mm²). The mean SPR response of the multiplex sensor for BSA and LYZ immediately after buffer washing is reported in the Supporting Information (Table S2).

For the multiplex assays, freshly prepared standard solutions (PBS-T) containing a mixture of insulin, glucagon, and somatostatin were prepared. The optimal amount of antibodies was then added and gently mixed for 2 min before injecting into the SPR system. Figure 6 shows the calibration curves for multiplex sensing of insulin (blue), glucagon (red), and somatostatin (black). For each hormone, mean relative binding values (C/C_0) were plotted as a function of hormone concentration (ng/mL). During experiments, the mean SPR shift was measured in at least 3 spots for each hormone and the controls. Then, an average of these SPR shifts from 3 independent sensors was calculated, and the bars in Figure 6 represent the corresponding SD. The LOD and dynamic range

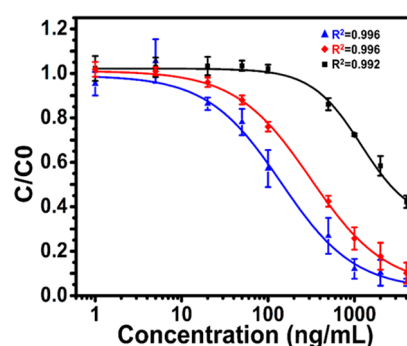


Figure 6. Multiplex hormone calibration curves in PBS-T for insulin (blue), glucagon (red), and somatostatin (black). For each hormone, mean relative binding values (C/C_0) were plotted as a function of hormone concentration (ng/mL). Relative binding was calculated by dividing the response of a range of standard solutions containing a mix hormones (C) by the response of the blank solution containing only a fixed concentration of antibodies (C_0). Solid lines correspond to the fitting of a nonlinear 4PL model. Error bars represent the standard deviation from 3 independent experiments ($n = 3$).

for multiplex immunoassays are shown in Table 3. Typical SPR curves for the multiplex detection mode can be found in the Supporting Information (Figures S3–S6).

Table 3. SPR Sensing Performance for Multiplexed Immunoassays^a

hormone	max ΔR (%) (C_0)	LOD (ng/mL)	LOD (nM)	dynamic range (ng/mL)
insulin	1.69 ± 0.02	8	1	34–633
glucagon	1.52 ± 0.01	14	4	85–1592
somatostatin	0.93 ± 0.03	403	246	719–4000 ^b

^aAll values were calculated from the nonlinear 4PL fit equation derived from individual calibration curves. The reported LOD was calculated as the response of the blank (C_0) minus 3 times the standard deviation.

^bHighest concentration tested.

The LOD of the sensor in multiplex mode was very similar to that of individual sensors. However, it can be noticed that the dynamic range for each hormone is different from each other. This could be as a result of variations in the hormones' surface density caused by the surface functionalization of the gold-coated prism outside of the SPR system.

Interestingly, the LOD of the SPR immunoassays in the multiplex mode were 1 order of magnitude higher than their corresponding ELISA assays (pg/mL). However, the high sensitivity of the ELISA method is not necessarily required for the detection of hormones directly secreted by a population of islets. For instance, previous reports demonstrated the individual detection of insulin¹³ and glucagon¹⁴ secreted (LOD) from 10 islets was 10 and 5 nM, respectively, at 15 mM glucose.

Since the number of somatostatin secreting cells within the islets is usually smaller than that of insulin or glucagon secreting cells,⁴ further protocol optimization could be required. Nevertheless, if the future detection of islet secretion products requires signal amplification, this could be readily addressed using gold nanoparticles, either within the sensing surface itself or as signal enhancing agent to increase the LOD of the present SPR immunoassays.⁴¹

CONCLUSIONS

In this work, we introduced a strategy for label-free and multiplex detection of pancreatic islet hormones with a LOD of 1 nM for insulin, 4 nM for glucagon, and 246 nM for somatostatin with a total analysis time per point of 21 min using a SPRi-based biosensor. The sensor showed comparable performance to previous reports where direct secretion of insulin and glucagon from a population of islets have been studied. The sensor exhibited excellent antifouling properties and specificity due to the design of a mixed SAM of a thiolated polyethylene glycol and 16-mercaptohexadecanoic acid showing a negligible response to a concentration of 1 mg/mL of BSA and a very little response to LYZ. This shows promise for the future operation of the sensor in a complex matrix such as a pancreatic islet secretome. The present SPRi-based biosensor could be easily integrated with previously developed microfluidic perfusion devices, which trap and reproduce the natural *in vivo* conditions of the islets, allowing real-time secretion analysis of pancreatic islet secretion. Such biosensing platform holds the potential to monitor a small islet's secretory fingerprint, allowing further understanding of the paracrine effect of somatostatin on glucose inducing insulin secretion as well as comprising a drug screening platform for the discovery of novel therapeutic agents for the treatment of diabetes.

ASSOCIATED CONTENT

Supporting Information

The Supporting Information is available free of charge on the ACS Publications website at DOI: [10.1021/acs.analchem.7b04288](https://doi.org/10.1021/acs.analchem.7b04288).

Quantitative data of nonspecific adsorption of BSA and LYZ on individual and multiplex mode and typical SPR curves for multiplex mode sensing (PDF)

AUTHOR INFORMATION

Corresponding Author

*E-mail: maryam.tabrizian@mcgill.ca.

ORCID

Maryam Tabrizian: 0000-0002-5050-4480

Notes

The authors declare no competing financial interest.

ACKNOWLEDGMENTS

The authors acknowledge the financial support from the Natural Science and Engineering Research Council of Canada (NSERC), the Fonds de Recherche Nature et Technologies-Team Grant, the NSERC-CREATE in ISS, and FRC scholarship from Consejo Nacional de Ciencia y Tecnología de México (CONACyT) and Secretaría de Educación Pública de México (SEP). The authors are also thankful to F. Melaine for her insightful discussions during the development of this work.

REFERENCES

- (1) International Diabetes Federation. OpenURL, 2015.
- (2) Hall, J. E.; Guyton, A. C. *Guyton and Hall Textbook of Medical Physiology*, 12th ed.; Saunders Elsevier: Philadelphia, PA, 2011.
- (3) Yovos, J. G. *Diabetes Res. Clin. Pract.* **2011**, *93*, S25–S26.
- (4) Cabrera, O.; Berman, D. M.; Kenyon, N. S.; Ricordi, C.; Berggren, P. O.; Caicedo, A. *Proc. Natl. Acad. Sci. U. S. A.* **2006**, *103* (7), 2334–2339.
- (5) Caicedo, A. *Semin. Cell Dev. Biol.* **2013**, *24* (1), 11–21.

- (6) Wierup, N.; Sundler, F.; Heller, R. S. *J. Mol. Endocrinol.* **2014**, *52* (1), R35–R49.
- (7) Braun, M. In *Pancreatic Beta Cell*; Litwack, G., Ed.; Elsevier Academic Press Inc: San Diego, CA, 2014; Vol. 95, pp 165–193.
- (8) Braun, M.; Ramracheya, R.; Johnson, P. R.; Rorsman, P. *Ann. N. Y. Acad. Sci.* **2009**, *1152* (1), 187–193.
- (9) Hanna, S. T.; Pigeau, G. M.; Galvanovskis, J.; Clark, A.; Rorsman, P.; MacDonald, P. E. *Pfluegers Arch.* **2009**, *457* (6), 1343–1350.
- (10) Luciani, D. S.; Johnson, J. D. *Mol. Cell. Endocrinol.* **2005**, *241* (1), 88–98.
- (11) Braun, M.; Ramracheya, R.; Bengtsson, M.; Clark, A.; Walker, J. N.; Johnson, P. R.; Rorsman, P. *Diabetes* **2010**, *59* (7), 1694–1701.
- (12) Ramracheya, R.; Ward, C.; Shigeto, M.; Walker, J. N.; Amisten, S.; Zhang, Q.; Johnson, P. R.; Rorsman, P.; Braun, M. *Diabetes* **2010**, *59* (9), 2198–2208.
- (13) Roper, M. G.; Shackman, J. G.; Dahlgren, G. M.; Kennedy, R. T. *Anal. Chem.* **2003**, *75* (18), 4711–4717.
- (14) Shackman, J. G.; Reid, K. R.; Dugan, C. E.; Kennedy, R. T. *Anal. Bioanal. Chem.* **2012**, *402* (9), 2797–2803.
- (15) Lomasney, A. R.; Yi, L.; Roper, M. G. *Anal. Chem.* **2013**, *85* (16), 7919–7925.
- (16) Castiello, F. R.; Heileman, K.; Tabrizian, M. *Lab Chip* **2016**, *16* (3), 409–431.
- (17) Xing, Y.; Nourmohammadzadeh, M.; Elias, J. E. M.; Chan, M. W.; Chen, Z. Q.; McGarrigle, J. J.; Oberholzer, J.; Wang, Y. *Biomed. Microdevices* **2016**, *18* (5), 9.
- (18) Lee, D.; Wang, Y.; Mendoza-Elias, J. E.; Adewola, A. F.; Harvat, T. A.; Kinzer, K.; Gutierrez, D.; Qi, M.; Eddington, D. T.; Oberholzer, J. *Biomed. Microdevices* **2012**, *14* (1), 7–16.
- (19) Proks, P.; Eliasson, L.; Ammälä, C.; Rorsman, P.; Ashcroft, F. M. *J. Physiol.* **1996**, *496* (1), 255–264.
- (20) Yang, L.; Ji, W.; Xue, Y.; Chen, L. *J. Mol. Med.* **2013**, *91* (8), 929–938.
- (21) Süß, C.; Solimena, M. *Exp. Clin. Endocrinol. Diabetes* **2008**, *116* (S 01), S13–S20.
- (22) Li, Y. V. *Endocrine* **2014**, *45* (2), 178–189.
- (23) Rorsman, P.; Braun, M. *Annu. Rev. Physiol.* **2013**, *75*, 155–179.
- (24) Singh, P. *Sens. Actuators, B* **2016**, *229*, 110–130.
- (25) Nault, L.; Guo, P.; Jain, B.; Brechet, Y.; Bruckert, F.; Weidenhaupt, M. *Acta Biomater.* **2013**, *9* (2), 5070–5079.
- (26) Hiep, H. M.; Nakayama, T.; Saito, M.; Yamamura, S.; Takamura, Y.; Tamiya, E. *Jpn. J. Appl. Phys.* **2008**, *47* (2), 1337–1341.
- (27) Grasso, G.; Bush, A. I.; D'Agata, R.; Rizzarelli, E.; Spoto, G. *Eur. Biophys. J.* **2009**, *38* (4), 407–414.
- (28) Gao, J.; Tong, H.; Huang, Z.; Liu, R.; Li, X.; Qiang, O.; Tang, C. *Anal. Methods* **2013**, *5* (13), 3201–3206.
- (29) Lerch, M.; Kamimori, H.; Folkers, G.; Aguilar, M. I.; Beck-Sickinger, A. G.; Zerbe, O. *Biochemistry* **2005**, *44* (25), 9255–9264.
- (30) Zou, C.; Kumaran, S.; Markovic, S.; Walsler, R.; Zerbe, O. *ChemBioChem* **2008**, *9* (14), 2276–2284.
- (31) Takagi, K.; Legrand, R.; Asakawa, A.; Amitani, H.; François, M.; Tenoune, N.; Coëffier, M.; Claeysens, S.; Do Rego, J. C.; Déchelotte, P.; Inui, A.; Fetissov, S. O. *Nat. Commun.* **2013**, *4*, 2685.
- (32) Love, J. C.; Estroff, L. A.; Kriebel, J. K.; Nuzzo, R. G.; Whitesides, G. M. *Chem. Rev.* **2005**, *105* (4), 1103–1169.
- (33) Gobi, K. V.; Iwasaka, H.; Miura, N. *Biosens. Bioelectron.* **2007**, *22* (7), 1382–1389.
- (34) Estevez, M. C.; Belenguer, J.; Gomez-Montes, S.; Miralles, J.; Escuela, A. M.; Montoya, A.; Lechuga, L. M. *Analyst* **2012**, *137* (23), 5659–5665.
- (35) Biacore Life Sciences, GE Healthcare, Uppsala, Sweden, 2003.
- (36) Mitchell, J. *Sensors* **2010**, *10* (8), 7323–7346.
- (37) Vaisocherova, H.; Brynda, E.; Homola, J. *Anal. Bioanal. Chem.* **2015**, *407* (14), 3927–3953.
- (38) Mitchell, J. S.; Wu, Y.; Cook, C. J.; Main, L. *Steroids* **2006**, *71* (7), 618–631.
- (39) Cui, X.; Yang, F.; Sha, Y.; Yang, X. *Talanta* **2003**, *60* (1), 53–61.
- (40) Haasnoot, W.; Gerçek, H.; Cazemier, G.; Nielen, M. W. F. *Anal. Chim. Acta* **2007**, *586* (1), 312–318.

(41) Bedford, E. E.; Spadavecchia, J.; Pradier, C. M.; Gu, F. X. *Macromol. Biosci.* **2012**, *12* (6), 724–739.